HHS Public Access

Author manuscript

Nat Med. Author manuscript; available in PMC 2012 September 01.

Published in final edited form as:

Nat Med. ; 18(3): 446–451. doi:10.1038/nm.2649.

A Quantitative Basis for Antiretroviral Therapy for HIV-1 Infection

Benjamin L. Jilek[1], **Melissa Zarr**[2], **Maame E. Sampah**[1], **S. Alireza Rabi**[1], **Cynthia K. Bullen**[1], **Jun Lai**[1], **Lin Shen**[1,2], and **Robert F. Siliciano**[1,2,3]

[1]Departments of Medicine, Baltimore MD

[2]Departments of Pharmacology and Molecular Sciences, Baltimore MD

[3]Departments of Johns Hopkins University School of Medicine, and Howard Hughes Medical Institute, Baltimore MD

Abstract

Highly active antiretroviral therapy (HAART)[1–3] has dramatically decreased mortality from HIV-1 infection[4] and is a major achievement of modern medicine. However, there is no fundamental theory of HAART. Elegant models describe the dynamics of viral replication[3,5–9], but a metric for the antiviral activity of drug combinations relative to a target value needed for control of replication is lacking. Treatment guidelines[10,11] are based on empirical results of clinical trials in which other factors like regimen tolerability also affect outcome. Why only certain drug combinations control viral replication remains unclear.

Here we quantify the intrinsic antiviral activity of antiretroviral drug combinations. We show that most single antiretrovirals exhibit previously unappreciated complex non-linear pharmacodynamics that determine their inhibitory potential at clinical concentrations. We demonstrate that neither of the major theories for drug combinations accurately predicts the combined effects of multiple antiretrovirals. However, combined effects can be understood with a novel approach that considers the degree of independence of drug effects.

This analysis allows a direct comparison of the inhibitory potential of different drug combinations under clinical concentrations, reconciles the results of clinical trials, defines a target level of inhibition associated with treatment success, and provides a rational basis for treatment simplification and optimization.

Standard dose-response curves for antiviral drugs, which plot the fraction of infection events unaffected by drug (f_u) against log of drug concentration (log D), obscure the slope parameter (m), a measure of curve steepness. Slope strongly influences antiviral acticity[12] and is part of all fundamental pharmacodynamic equations[13–15] including the median-effect equation[16]:

Author contributions

B.L.J., M.Z., M.E.S., C.K.B., and J.L. conducted the experiments. B.L.J., M.Z., S.A.R., L.S., and R.F.S carried out the computational analysis. R.F.S. supervised the project and wrote the manuscript.

$$f_u = \frac{1}{1+\left(\frac{D}{IC_{50}}\right)^m} \quad (1)$$

or

$$log\ [(1 - f_u)/f_u] = m\ logD - m\ logIC_{50} \quad (2)$$

Equation 2 linearizes dose-response curves such that a logarithmic measure of inhibition, log [(1−f_u)/f_u], increases linearly with log D (Fig. 1a). The slope of the line is m. For log [(1−f_u)/f_u)] > 2, log [(1−f_u)/f_u)] ≈ log (1/f_u), the instantaneous inhibitory potential (*IIP*), a useful measure of antiviral activity[12]. *IIP* is the number of logs single round infection events are reduced by a drug. Drugs with high m produce much more inhibition (Fig. 1a).

The influence of m is apparent in HIV-1 infectivity assays[12,17] with different drugs. For the integrase strand transfer inhibitor (InSTI) raltegravir (RAL), $m \approx 1$ (Fig. 1b). At C_{max}, RAL produces ~2 logs inhibition (*IIP* ≈ 2). Curves for the protease inhibitor (PI) atazanavir (ATV) are steeper and strikingly non-linear (Fig. 1c). An upward inflection dramatically increases inhibition for minor increases in D (Supplementary Note 1, Fig. S1, Table S1). Inhibition at clinical concentrations can only be estimated by extrapolation from the upper end of the observable range (Fig. 1c, Supplementary Note 2, Fig. S2). At C_{max}, ATV produces ~8 logs of inhibition. Similar analysis showed that most antiretrovirals have complex, non-linear median-effect plots (Fig. 1d, Supplementary Table S1). Different drugs showed highly significant differences in slope at clinical concentrations (m') (Supplementary Table S2). Grouping curves by drug class and normalizing by IC_{50} revealed that all PIs and non-nucleoside RT inhibitors (NNRTIs) have steep, upwardly inflected curves, with maximum m > 3 and > 2, respectively (Fig. 1e, Supplementary Table S1). These complex curves may reflect intermolecular cooperativity[18]. Complex curves were observed for several other antiretrovirals (Fig. 1e, Supplementary Note 3). These results reveal unappreciated complexities in dose-response relationships for antiretrovirals.

To demonstrate how these curves behave in the clinical range, concentrations were normalized by C_{max} (Fig. 1f). For the PIs ATV, darunavir (DRV), and lopinavir (LPV), and the NNRTI efavirenz (EFV), curves inflect upward at $D < C_{min}$, giving extraordinarily high *IIP* at clinical concentrations, consistent with clinical trial results[10,11]. For the PI nelfinavir (NFV), the inflection occurs at $D > C_{min}$ (Fig. 1f), explaining its inferior clinical performance[19]. Because the PI ritonavir (RTV) is used at low concentrations to “boost” other PIs, its curve inflects at the top of the clinical range, providing little antiviral activity. Thus understanding the complex shapes of dose-response curves at clinical concentrations is critical for assessing antiviral activity.

Pharmacokinetics are also important[12]. We computed the average *IIP* over the dosing interval (IIP_{ave}) from the area under the *IIP* vs. time curve to allow quantitative comparison of antiviral activity of different drugs at expected plasma concentrations (Fig. 1g, Supplementary Tables S3,S4). IIP_{ave} in tissue sites that have different drug concentrations than plasma could be similarly estimated provided the relevant pharmacokinetic data were

available. Overall, the results explain the established clinical value of NNRTIs and PIs[10,11]. Steep, upwardly inflected curves allow these drugs to achieve extremely high IIP_{ave}. We previously estimated that 10^6 infection events occur per viral generation in the average untreated patient, suggesting that $IIP_{ave} > 6$ would be required to immediately halt replication[20]. Only NNRTIs and PIs approach this level. The PI DRV has the highest IIP_{ave}. PIs are the only class for which monotherapy has had success[21–23]. Conventional dose-response curves obscure differences in *IIP* (Fig. 1g, inset).

Some drugs with low IIP_{ave} like RAL and MVC are effective in combination therapy[24,25]. We hypothesized that these drugs might have favorable or synergistic interactions in combinations, compensating for low intrinsic IIP_{ave}. Two fundamental models describe combined effects[26,27] (Fig. 2a). Bliss independence[28] assumes independent action such that the combined effect (f_{u1+2}) is the product of the fractions unaffected by each drug:

$$f_{u_{1+2}} = f_{u_1} \times f_{u_2} = \frac{1}{1+\left(\frac{D_1}{IC_{50_1}}\right)^{m_1}} \times \frac{1}{1+\left(\frac{D_2}{IC_{50_2}}\right)^{m_2}} \quad (3)$$

Loewe additivity[29] is based on isobolograms and assumes similar mechanisms or competition for the same binding site. For positive inhibitory slopes, Loewe additivity is described by Equation 4:

$$1 = \frac{D_1}{IC_{50_1}\left(\frac{f_{u_{1+2}}}{1-f_{u_{1+2}}}\right)^{-1/m_1}} + \frac{D_2}{IC_{50_2}\left(\frac{f_{u_{1+2}}}{1-f_{u_{1+2}}}\right)^{-1/m_2}} \quad (4)$$

Bliss independence predicts higher inhibition, with upwardly inflected curves (Fig. 2b). There has been no systematic evaluation of which model applies to antiretrovirals. Therefore, we analyzed 166 of 171 possible pairwise combinations of 19 commonly used antiretrovirals.

Experimental inhibition unambiguously fit one of the standard models for < 60% of combinations (Supplementary Fig. S3). Intermediate inhibition was common and can be understood by considering NRTI-NNRTI interactions. Although these classes bind different sites, they inhibit the same process and are not fully independent. The inhibition produced by a given combination showed a consistent relationship to predictions of the two models as drug concentrations increased (Fig. 2c). This suggests that combinations can be characterized on a spectrum defined by two states, independent inhibition (Bliss) and competitive binding (Loewe), with synergistic and antagonistic interactions at either extreme. To quantify degree of independence (*DI*), we developed a novel index with combinations following Loewe additivity assigned *DI* = 0 and combinations following Bliss independence assigned *DI* = 1. The index is computed as:

$$DI = \frac{F_E - F_L}{F_B - F_L} \quad (5)$$

where F_E, F_L, and F_B are logarithmic measures of inhibition, $\log[(1-f_u)/f_u]$, for the experimental data, and Loewe and Bliss predictions, respectively (Fig. 2c). This approach

incorporates both classic models and maps inhibition on a median-effect plot in relation to the models.

Representative combination experiments are shown in Fig. 2d. Expected results based the competitive binding criterion are in Fig. 2e. Experimental results, categorized by *DI* index, are in Fig. 2f and Supplementary Table S5. Some combinations targeting different steps in the life cycle followed Bliss independence and showed higher combined effects. This is illustrated by the InSTI-NRTI combination RAL-FTC (Fig. 2d, R^2=0.99 for Bliss) and was observed for combinations of InSTIs with drugs from all other classes (Fig. 2f). The excellent clinical performance of InSTI-based regimens[24] may reflect these favorable interactions. The chemokine receptor antagonist maraviroc (MVC) also showed favorable interactions (Fig. 2f).

Drugs binding to the same site, such as the hydrophobic NNRTI pocket[30], should follow Loewe additivity. This is illustrated by the NNRTI-NNRTI combination etravirine (ETR)-nevirapine (NVP) (R^2=0.99 and 0.64 for Loewe and Bliss, respectively). Loewe additivity was observed for combinations of two NNRTIs, two InSTIs, and two nucleoside analogs of the same base (AZT-d4T, 3TC-FTC, and ddI-TDF) (Fig. 2f). The AZT-d4T combination is considered antagonistic due to effects at the level of phosphorylation[31] and suboptimal clinical responses[32]. However, in infectivity assays, this combination fits the Loewe prediction perfectly (R^2=0.99). All PI pairs showed inhibition greater than the Loewe predictions, perhaps reflecting the effects of protease inhibition on multiple downstream steps in the life cycle[33,34,35].

Another common pattern was a combined effect between the Bliss and Loewe predictions, reflecting some lack of independence. This is illustrated by the NRTI-NNRTI combination ABC-NVP (Fig. 2d). Intermediate effects were observed for many RTI-PI combinations and some RTI-RTI and PI-PI combinations (Fig. 2f, Supplementary Table S5, Supplementary Fig. S4) As discussed above, lack of independence is expected for combinations of RTIs, and, for PI-RTI combinations, may represent effects of incomplete maturation on downstream events in the life cycle[33,34,35]. Combined effects significantly greater than the Bliss prediction represent synergy and were observed for combinations of deoxythymidine analogs zidovidine (AZT) or stavudine (d4T) with other RTIs (Fig. 2d, AZT-NVP) and for certain other combinations (Fig. 2f). Together, these results suggest that degree of independence of two drugs has a major impact on the combined effect.

IIP for triple combinations (IIP_{1+2+3}) can be estimated using three drug versions of the Bliss and Loewe models, with Bliss independence predicting higher combined effects (Fig. 3). Antagonism, defined as inhibition less than the Loewe prediction, was uncommon in pairwise analysis (Fig. 2f). Therefore, we assume that the lower bound of IIP_{1+2+3} is the Loewe prediction. Similarly, since most two drug combinations showed inhibition less than or equal to the Bliss prediction, the upper bound of IIP_{1+2+3} is the Bliss prediction except for cases in which strong synergistic interactions dominate. Using these bounds, we determined the range of $IIP_{ave1+2+3}$ for all three drug combinations of 19 commonly used antiretrovirals (Fig. 4a). Because the Bliss and Loewe predictions diverge with increasing *D* (Fig. 2b, 3b), the ranges are broad. Predicted $IIP_{ave1+2+3}$ values for different regimens vary

dramatically. At the high end are regimens with two drugs whose dose-response curves inflect sharply upward at $D < C_{min}$ (e.g. EFV+DRV). At the low end are dual-NRTI regimens. To examine the relationship between $IIP_{ave1+2+3}$ and clinical outcome, we estimated $IIP_{ave1+2+3}$ more precisely using a weighted average of the relevant pairwise *DI* values (Fig. 4, Supplementary Table S6). By accounting for different modes of pairwise interaction, this approach gives better agreement with experimentally determined $IIP_{ave1+2+3}$ than either the Loewe or Bliss models (Supplementary Fig. S5, Supplementary Table S7). Despite the complicating factor of regimen tolerability, predictions of $IIP_{ave1+2+3}$ based on *DI* index values correlated well with outcome (Supplementary Figure S6, correlation coefficient=0.686, $P < 0.001$). Only 1 of 31 evaluated regimens with $IIP_{ave1+2+3} < 8$ had > 70% of patients with a viral load < 50 copies/ml at 48 weeks. Among evaluated regimens meeting this criterion, the one with the lowest $IIP_{ave1+2+3}$ was TDF+FTC+RAL[36]. Using *DI* values, we estimate an $IIP_{ave1+2+3}$ of 5.05 for this regimen. This is at the high end of the Loewe-Bliss range due to favorable RAL interactions (Fig. 4b). These results suggest that 5–8 logs of inhibition are required for successful HAART. The triple NRTI regimen TDF+3TC+ABC had a similar Loewe-Bliss range but inferior efficacy[37], possibly because the actual $IIP_{ave1+2+3}$ value is closer to the low end of the Loewe-Bliss range (due to low *DI* for ABC pairs) and below the 5 log threshold (Fig. 4b). Three of the other regimens currently recommended for initial treatment had $IIP_{ave1+2+3} > 5$ due primarily to the *IIP* of the base drug (EFV, ATV/r, DRV/r). Above $IIP_{ave1+2+3} = 7$, there was little correlation with outcome (correlation coefficient = 0.125, $P = 0.29$) because at this level, replication is essentially halted, and outcome depends mainly on adherence.

This approach provides a quantitative basis for HAART. HAART controls viral replication because of steep, upwardly infected dose-response curves for some drugs and synergies reflecting the independent action for other drugs. Despite high inhibitory potential, it is not curative because of stable reservoirs[38,39]. This approach also permits a comprehensive search for regimens with suprathreshold antiviral activity, maximum tolerability, and minimum cost. Simpler two or three drug regimens with adequate *IIP* but lower cost and toxicity may be important for extending therapy in resource-limited settings. Finally, this approach may allow more rational selection of salvage regimens.

Methods

We measured drug inhibition of HIV-1 infection using a single round infectivity assay as previously described[12,17]. We chose a single round assay because complex factors such as growth and death of target cells distort *m* in multiround assays[40]. To accurately mimic infection events *in vivo*, we carried out infections in primary $CD4^+$ T lymphoblasts obtained by PHA activation of peripheral blood mononuclear cells from health donors as previously described[17]. All blood donors provided informed consent according to a protocol approved by the Johns Hopkins Institutional Review Board. We infected $CD4^+$ T lymphoblasts with recombinant HIV-1 pseudoviruses generated by transfection of HEK 293 T cells with a previously described[12] HIV-1 vector (pNL43-ΔE-EGFP) containing a GFP-tagged, defective envelope. The envelope was provided in *trans* by co-transfection with an envelope expression vector. In most cases, we used a CXCR4-tropic envelope (HXB2) because it gave higher level infection of primary $CD4^+$ T lymphoblasts, thus affording a wider

dynamic range. However, IC_{50}' and m' values obtained in infections with CCR5-tropic pseudoviruses were not significantly different from those obtained with CXCR4-tropic viruses (Supplementary Table S8), and modes of drug interaction were also similar (Supplementary Table S7). To account for individual variation in cellular uptake and metabolism of drugs, we performed replicate assays in lymphoblasts from 10–60 donors for each drug and computed average levels of inhibition. We used high serum concentrations (55%) to account for protein binding. For protein bound drugs, titrations of drug effect vs. serum concentration demonstrated that inclusion of 50% human serum and 5% fetal calf serum provided a close approximation for *in vivo* drug binding. We pretested lots of human serum for low toxicity to $CD4^+$ T lymphoblasts. Drugs were added to lymphoblast targets, and cells were incubated at 37°C for 16 hours before infection to allow sufficient time for triphosphorylation of NRTIs. Longer preincubations did not enhance antiviral activity. PIs were also added at the stage of virus production in 293T cells[17]. After spin infection in 96 well plates, targets incubated for 3 days at 37°C. Cells were then fixed in 2% formaldehyde, and GFP expression was analyzed by flow cytometry. After gating for viable cells, the fraction of infection events unaffected by drug (f_u) was determined as the % GFP^+ cells in the presence of drug divided by the % GFP^+ cells in control wells without drug. Calculation of *IIP* from f_u is described in Supplementary Material, Methods.

To determine whether the combined effect of two antiretroviral drugs followed the predictions of the Bliss or Loewe models, we tested pairs of drugs at constant molar ratios chosen to maximize the difference between the levels of inhibition predicted by the two models. Drug combinations are often evaluated in surface experiments in which all possible combinations of several different concentrations of each drug are tested[26,27]. However, the difference between the inhibition predicted by the two models increases with drug concentration (Fig. 2b) and is maximal when both drugs contribute equally to the observed suppression (R. Siliciano, unpublished observation). Therefore, we chose drug concentrations such that at the highest concentrations used, the total inhibition predicted by the Bliss model would be within the dynamic range of the assay (*IIP* < 3), with each drug contributing equally. Drugs were mixed at these concentrations and serially diluted. Experimental analysis was carried out in cells from 5–15 donors/combination as described above. PIs were added at the virus production stage. Analysis of combination experiments is described in Supplementary Material, Methods.

Supplementary Material

Refer to Web version on PubMed Central for supplementary material.

Acknowledgements

We thank Drs. J. Blankson, A. Spivak, C. Durand, J. Gallant, J. Cofrancesco, and W. Greco for helpful discussions. This work was supported by US National Institutes of Health grant AI081600 and by the Howard Hughes Medical Institute.

References

1. Gulick RM, et al. Treatment with indinavir, zidovudine, and lamivudine in adults with human immunodeficiency virus infection and prior antiretroviral therapy. N. Engl. J. Med. 1997; 337:734–739. [PubMed: 9287228]
2. Hammer SM, et al. A controlled trial of two nucleoside analogues plus indinavir in persons with human immunodeficiency virus infection and CD4 cell counts of 200 per cubic millimeter or less. AIDS Clinical Trials Group 320 Study Team. N. Engl. J. Med. 1997; 337:725–733. [PubMed: 9287227]
3. Perelson AS, et al. Decay characteristics of HIV-1-infected compartments during combination therapy. Nature. 1997; 387:188–191. [PubMed: 9144290]
4. Walensky RP, et al. The survival benefits of AIDS treatment in the United States. J. Infect. Dis. 2006; 194:11–19. [PubMed: 16741877]
5. Wei X, et al. Viral dynamics in human immunodeficiency virus type 1 infection. Nature. 1995; 373:117–122. [PubMed: 7529365]
6. Ho DD, et al. Rapid turnover of plasma virions and CD4 lymphocytes in HIV-1 infection. Nature. 1995; 373:123–126. [PubMed: 7816094]
7. Coffin JM. HIV population dynamics in vivo: implications for genetic variation, pathogenesis, and therapy. Science. 1995; 267:483–489. [PubMed: 7824947]
8. Perelson AS, Neumann AU, Markowitz M, Leonard JM, Ho DD. HIV-1 dynamics in vivo: virion clearance rate, infected cell life-span, and viral generation time. Science. 1996; 271:1582–1586. [PubMed: 8599114]
9. Wodarz D, Nowak MA. Mathematical models of HIV pathogenesis and treatment. Bioessays. 2002; 24:1178–1187. [PubMed: 12447982]
10. Thompson MA, et al. Antiretroviral treatment of adult HIV infection: 2010 recommendations of the International AIDS Society-USA panel. JAMA. 2010; 304:321–333. [PubMed: 20639566]
11. Panel on Antiretroviral Guidelines for Adults and Adolescents. Guidelines for the use of antiretroviral agents in HIV-1-infected adults and adolescents; Department of Health and Human Services. 2009. p. 1-161.Available at http://www.aidsinfo.nih.gov/ContentFiles/AdultandAdolescentGL.pdf
12. Shen L, et al. Dose-response curve slope sets class-specific limits on inhibitory potential of anti-HIV drugs. Nat. Med. 2008; 14:762–766. [PubMed: 18552857]
13. Hill AV. The possible effects of the aggregation of the molecules of huemoglobin on its dissociation curves. J. Physiol. (London). 1910; 40:iv–vii.
14. Chou TC. Derivation and properties of Michaelis-Menten type and Hill type equations for reference ligands. J. Theor. Biol. 1976; 59:253–276. [PubMed: 957690]
15. Holford NH, Sheiner LB. Understanding the dose-effect relationship: clinical application of pharmacokinetic-pharmacodynamic models. Clin. Pharmacokinet. 1981; 6:429–453. [PubMed: 7032803]
16. Chou TC, Talalay P. Quantitative analysis of dose-effect relationships: the combined effects of multiple drugs or enzyme inhibitors. Adv. Enzyme Regul. 1984; 22:27–55. [PubMed: 6382953]
17. Sampah ME, Shen L, Jilek BL, Siliciano RF. Dose-response curve slope is a missing dimension in the analysis of HIV-1 drug resistance. Proc. Natl. Acad. Sci. U. S. A. 2011; 108:7613–7618. [PubMed: 21502494]
18. Shen L, et al. A critical subset model provides a conceptual basis for the high antiviral activity of major HIV drugs. Sci. Transl. Med. 2011; 3:91ra63.
19. Walmsley S, et al. Lopinavir-ritonavir versus nelfinavir for the initial treatment of HIV infection. N. Engl. J. Med. 2002; 346:2039–2046. [PubMed: 12087139]
20. Siliciano JD, Siliciano RF. Biomarkers of HIV replication. Curr. Opin. HIV. AIDS. 2010; 5:491–497. [PubMed: 20978392]
21. Katlama C, et al. Efficacy of darunavir/ritonavir maintenance monotherapy in patients with HIV-1 viral suppression: a randomized open-label, noninferiority trial, MONOI-ANRS 136. AIDS. 2010; 24:2365–2374. [PubMed: 20802297]

22. Perez-Valero I, Arribas JR. Protease inhibitor monotherapy. Curr. Opin. Infect. Dis. 2011; 24:7–11. [PubMed: 21150592]
23. Bierman WF, van Agtmael MA, Nijhuis M, Danner SA, Boucher CA. HIV monotherapy with ritonavir-boosted protease inhibitors: a systematic review. AIDS. 2009; 23:279–291. [PubMed: 19114854]
24. Markowitz M, et al. Rapid and durable antiretroviral effect of the HIV-1 Integrase inhibitor raltegravir as part of combination therapy in treatment-naive patients with HIV-1 infection: results of a 48-week controlled study. J. Acquir. Immune Defic. Syndr. 2007; 46:125–133. [PubMed: 17721395]
25. Cooper DA, et al. Maraviroc versus efavirenz, both in combination with zidovudine-lamivudine, for the treatment of antiretroviral-naive subjects with CCR5-tropic HIV-1 infection. J. Infect. Dis. 2010; 201:803–813. [PubMed: 20151839]
26. Greco WR, Bravo G, Parsons JC. The search for synergy: a critical review from a response surface perspective. Pharmacol. Rev. 1995; 47:331–385. [PubMed: 7568331]
27. Chou TC. Theoretical basis, experimental design, and computerized simulation of synergism and antagonism in drug combination studies. Pharmacol. Rev. 2006; 58:621–681. [PubMed: 16968952]
28. Bliss CI. The toxicity of poisons jointly applied. Ann. Appl. Biol. 1939; 26:585–615.
29. Loewe S, Muischnek H. Effect of combinations: mathematical basis of problem. Arch. Exp. Pathol. Pharmakol. 1926; 114:313–326.
30. Kohlstaedt LA, Wang J, Friedman JM, Rice PA, Steitz TA. Crystal structure at 3.5 A resolution of HIV-1 reverse transcriptase complexed with an inhibitor. Science. 1992; 256:1783–1790. [PubMed: 1377403]
31. Hoggard PG, Kewn S, Barry MG, Khoo SH, Back DJ. Effects of drugs on 2',3'-dideoxy-2',3'-didehydrothymidine phosphorylation in vitro. Antimicrob. Agents Chemother. 1997; 41:1231–1236. [PubMed: 9174176]
32. Havlir DV, et al. In vivo antagonism with zidovudine plus stavudine combination therapy. J. Infect. Dis. 2000; 182:321–325. [PubMed: 10882616]
33. Wyma DJ, et al. Coupling of human immunodeficiency virus type 1 fusion to virion maturation: a novel role of the gp41 cytoplasmic tail. J. Virol. 2004; 78:3429–3435. [PubMed: 15016865]
34. Murakami T, Ablan S, Freed EO, Tanaka Y. Regulation of human immunodeficiency virus type 1 Env-mediated membrane fusion by viral protease activity. J. Virol. 2004; 78:1026–1031. [PubMed: 14694135]
35. Muller B, et al. HIV-1 Gag processing intermediates trans-dominantly interfere with HIV-1 infectivity. J. Biol. Chem. 2009; 284:29692–29703. [PubMed: 19666477]
36. Lennox JL, et al. Safety and efficacy of raltegravir-based versus efavirenz-based combination therapy in treatment-naive patients with HIV-1 infection: a multicentre, double-blind randomised controlled trial. Lancet. 2009; 374:796–806. [PubMed: 19647866]
37. Gallant JE, et al. Early virologic nonresponse to tenofovir, abacavir, and lamivudine in HIV-infected antiretroviral-naive subjects. J. Infect. Dis. 2005; 192:1921–1930. [PubMed: 16267763]
38. Finzi D, et al. Identification of a reservoir for HIV-1 in patients on highly active antiretroviral therapy. Science. 1997; 278:1295–1300. [PubMed: 9360927]
39. Finzi D, et al. Latent infection of CD4+ T cells provides a mechanism for lifelong persistence of HIV-1, even in patients on effective combination therapy. Nat. Med. 1999; 5:512–517. [PubMed: 10229227]
40. Ferguson NM, Fraser C, Anderson RM. Viral dynamics and anti-viral pharmacodynamics: rethinking in vitro measures of drug potency. Trends Pharmacol. Sci. 2001; 22:97–100. [PubMed: 11166854]

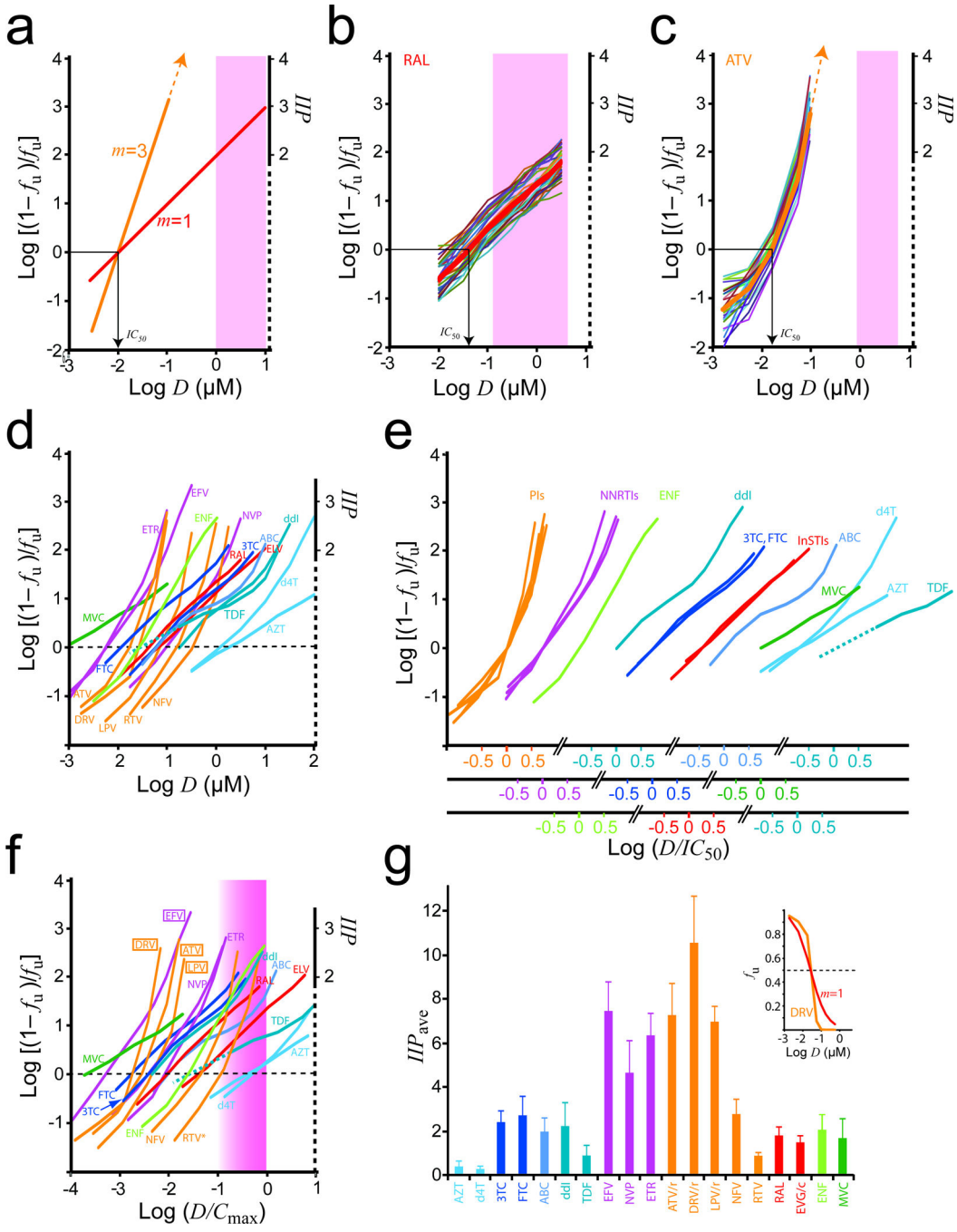

Figure 1.

Determining inhibitory potential from complex dose-response curves of antiretroviral drugs. **(a)** Median-effect plots for hypothetical drugs with m = 1 or 3 and the same IC_{50}. Clinical concentrations 100–1,000 × IC_{50} are assumed (shaded). **(b)** Dose-response curves RAL in primary CD4$^+$ T cells from 35 donors (thin lines) and mean curve (thick line). m = 0.98 ± 0.12. The clinical concentration range is shaded. **(c)** Dose-response curves for ATV. The clinical concentration range with standard dosing (*qd* with RTV) is shaded. **(d)** Mean dose-response curves for commonly used antiretroviral drugs. **(e)** Median-effect plots for classes

of antiretroviral drugs. Plots from (d) are grouped by drug class or subclass, and, within each group, normalized by IC_{50}. The deoxyadenosine analogs ddI and TDF have very different slopes in the clinical range and are plotted separately. **(f)** Median-effect plots normalized by C_{max}. The shaded area represents the approximate clinical concentration range, the lower end of which is not precisely defined here because the relationship between C_{min} and C_{max} varies for different drugs. However, except for NRTIs, clinical concentrations generally remain within a log of C_{max}. Where appropriate here and in Fig. 1g, values reflect concentrations achieved with pharmacokinetic boosting. For RTV, the 100 mg dose is assumed. **(g)** Mean IIP_{ave} ± SD for commonly used antiretrovirals. Conventional dose-response curves (f_u vs. log D) obscure the dramatic difference in the antiviral activity between a drug with a steep dose-response curve (DRV) and a hypothetical drug with the same IC_{50} and $m = 1$ (inset).

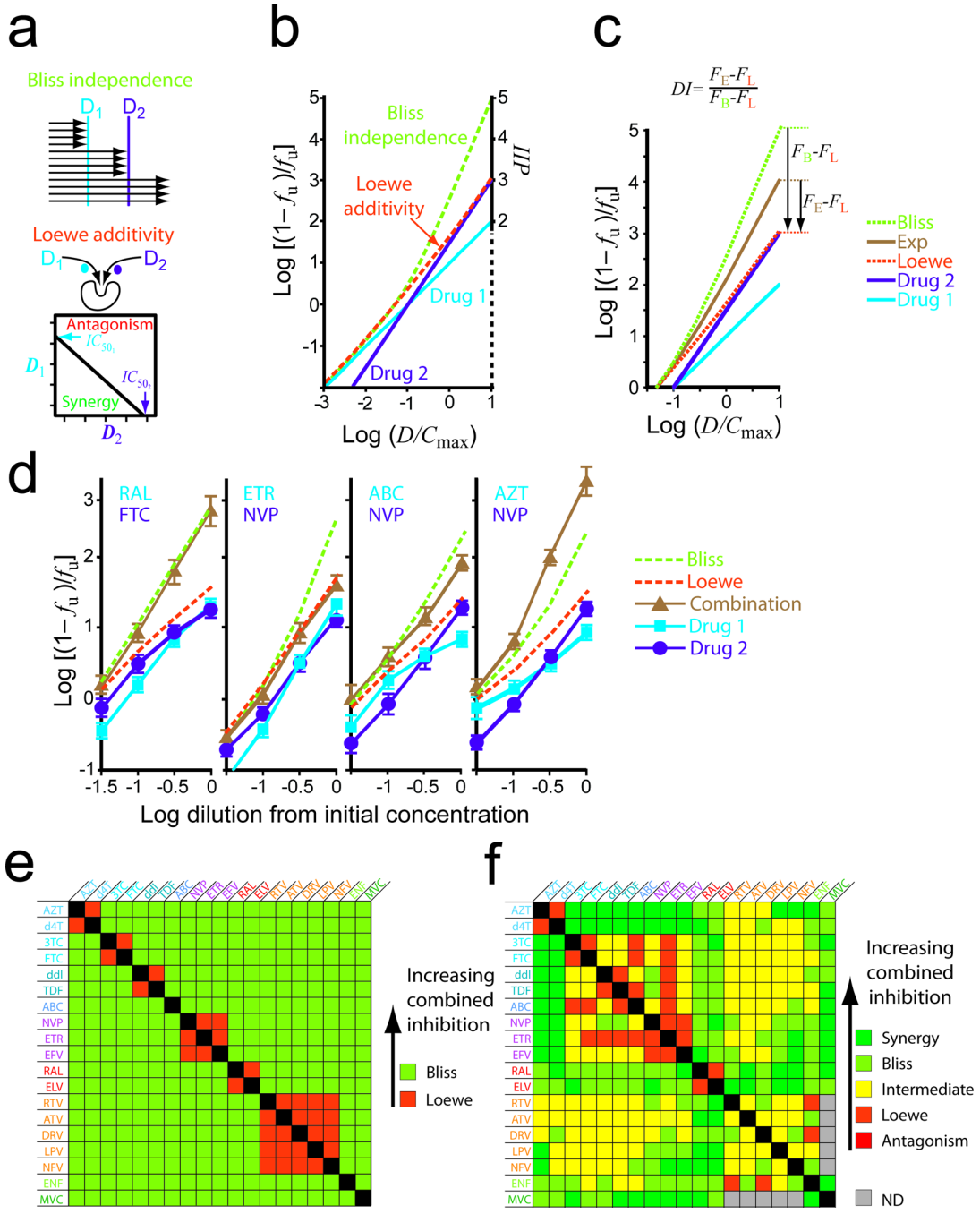

Figure 2.

Combined effects. **(a)** Bliss independence and Loewe additivity models for hypothetical drugs D_1 and D_2. Loewe additivity is based on isobolograms depicting the concentrations of D_1 and D_2 needed to produce 50% inhibition (black line). Deviations to the left or right reflect synergy or antagonism, respectively, if Loewe additivity is the model for combined effects. **(b)** Median-effect plots for D_1 and D_2 alone (solid lines) and predictions of the combined effects of D_1 + D_2 by the Bliss and Loewe models (dotted lines). D_1 and D_2 have slopes of 1 and 1.5, respectively, and are diluted in constant ratio from 10 × C_{max} which is

assumed to be 10 × IC_{50}. **(c)** Degree of independence (*DI*) index for quantifying experimental (Exp) combined effects in relations to the models. **(d)** Representative combination experiments. Drugs were diluted at constant ratio from initial concentrations chosen to maximize the differences between the Bliss and Loewe predictions (see Methods). The figures show experimental measurements for single drugs and combinations (solid lines) and the predictions of the models (dotted lines). These examples illustrate characteristic patterns of Bliss independence (RAL-FTC), Loewe additivity (ETR-NVP), intermediate effect (ABC-NVP), and synergy (AZT-NVP). **(e)** Expected combination effects based on the binding site criterion. **(f)** Observed combination effects categorized by *DI* values: synergy, $DI > 1.2$; Bliss, $0.8 < DI < 1.2$; intermediate, $0.2 < DI < 0.8$; Loewe, $-0.2 < DI < 0.2$, antagonism, $DI < -0.2$. Because of lower infection with R5-tropic pseudoviruses, PI-MVC combinations could not be analyzed. Individual variation in the combined effect was substantial for some combinations (Supplementary Figure S4).

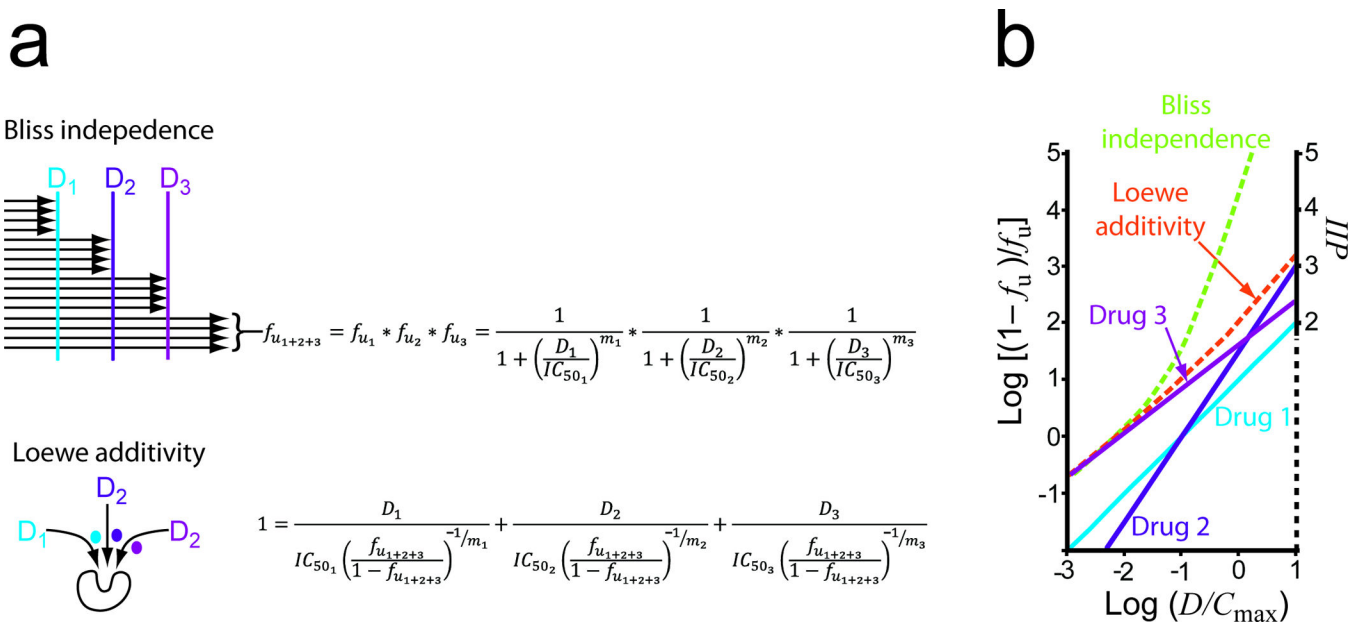

Figure 3.

Estimating the inhibitory potential of triple combinations. (**a**) Expansion of the Bliss and Loewe models to three drugs. The three drug Bliss formula is based on a simple extension of the idea that the fraction of viruses unaffected by the blocks imposed by three drugs acting at different steps in the life cycle (f_{u1+2+3}) is the product of the fraction unaffected by each drug. The Loewe formula is based on the idea the inhibitors act in a mutually exclusive way or compete for the same binding site as discussed by Chou[27]. It is derived from the general expression for an *n* drug combination with no synergy of antagonism as described in Supplementary Information, Methods. (**b**) Median-effect plots for hypothetical drugs D_1, D_2, and D_3 alone (solid lines) and predictions of the combined effects of D_1+D_2+ D_3 by the Bliss and Loewe models (dotted lines). D_1, D_2, and D_3 are diluted in constant ratio from 10 × C_{max} and assumed to have IC_{50} values of 0.1, 0.1, and 0.01 × C_{max} and slopes 1, 1.5, and 0.8, respectively.

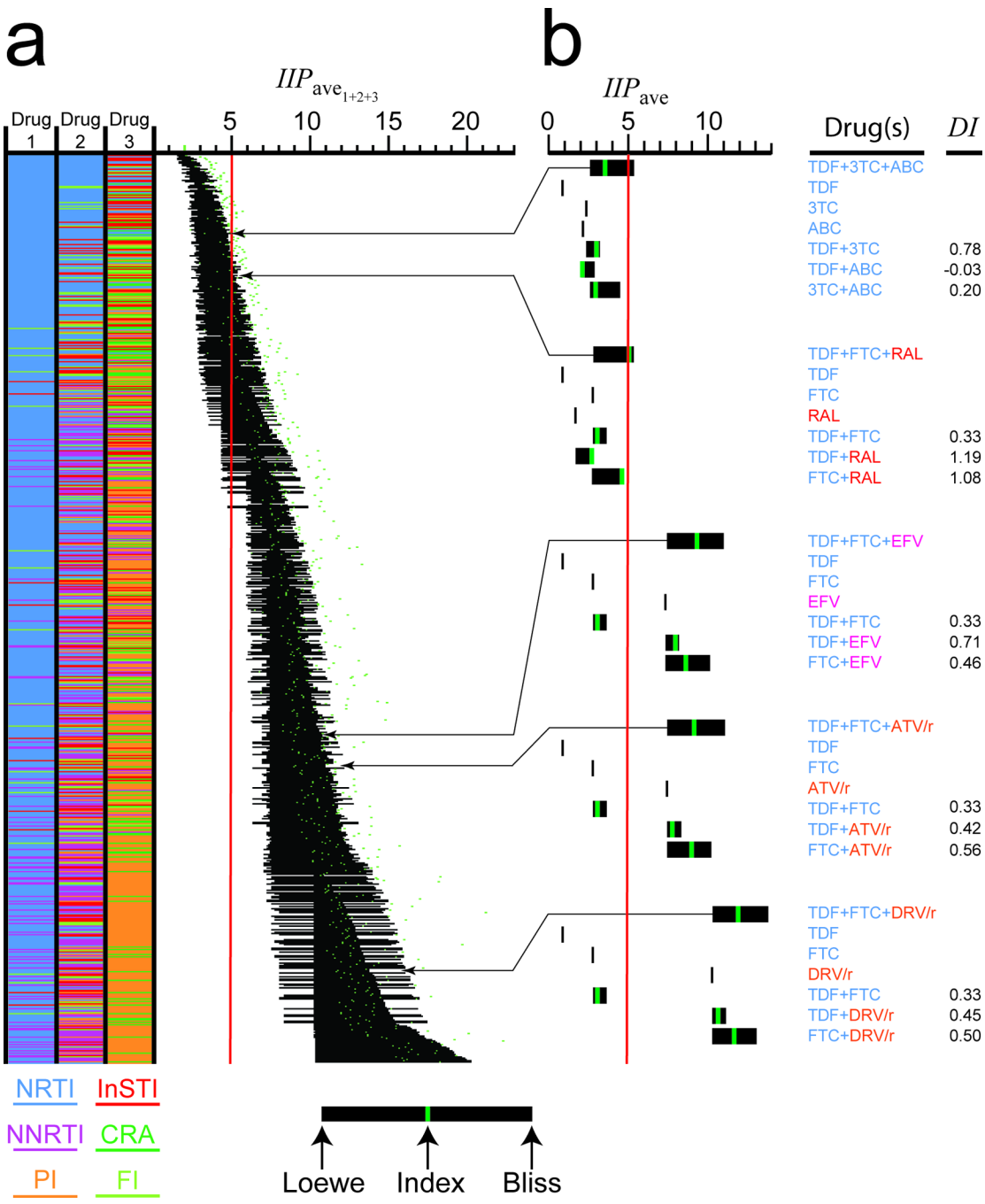

Figure 4.

Inhibitory potential of three drug combinations. **(a)** Estimated $IIP_{ave1+2+3}$ for triple combinations of 19 commonly used antiretroviralss. Combinations are color coded by drug class, excluding combinations with more than one drug from the NNRTI, PI, or InSTI classes, or NRTI subclasses. The black bars represent the range of estimated $IIP_{ave1+2+3}$ values with the Loewe prediction at the left and the Bliss prediction at the right. Regimens are sorted based on the midpoint of the range. An estimate based on the weighted average of the three pairwise *DI* index values is shown as a green dot. $IIP_{ave1+2+3}$ values above the

Loewe-Bliss range represent synergy, typically for regimens including thymidine analogues. The red line represents the minimum $IIP_{ave1+2+3}$ for a regimen achieving suppression of viremia in > 80% of patients. **(b)** Inhibitory potential of selected three drug combinations along with component single drugs and drug pairs. For combinations, inhibitory potential is shown as a range of $IIP_{ave1+2+3}$ values between the Loewe and Bliss predictions. For each component two drug combination, an estimate of IIP_{ave} based on experimentally determined *DI* index values is shown as a green bar. For three drug combinations, green bars represent estimates based on a weighted average of pairwise *DI* index values. Values are shown for currently recommended initial HAART regimens[10,11] and, for purposes of comparison, a suboptimal TDF+3TC+ABC regimen[37].